

# Three-family oscillations using neutrinos from muon beams at very long baseline

M. Campanelli<sup>1</sup>, A. Bueno<sup>1</sup>, A. Rubbia<sup>1,2</sup>

<sup>1</sup> *Institut für Teilchenphysik, ETHZ, CH-8093 Zürich, Switzerland*

<sup>2</sup> *CERN, Geneva, Switzerland*

## Abstract

The planned LBL experiments will be able to prove the hypothesis of flavor oscillation between muon and tau neutrinos. We explore the possibility of a second generation long baseline experiment at very long baselines, i.e.  $L$  in the range 6500 – 8800 km. This distance requires intense neutrino beams that could be available from very intense muon beams as those needed for  $\mu$  colliders. Such baselines allow to study neutrino oscillations with  $E/L \approx 2 \times 10^{-3} \text{ eV}^2$  with neutrinos of energy  $E_\nu \approx 20 \text{ GeV}$ , i.e. above tau threshold. Moreover, matter effects inside the Earth could lead to observable effects in  $\nu_e \rightarrow \nu_\mu$  oscillations. These effects are interchanged between neutrinos and antineutrinos, and therefore they can be tested by comparing the oscillated spectra obtained running the storage ring with positive and negative muons.

## 1 Introduction

The use of neutrinos from muon decays has several advantages:

- easy prediction of the neutrino fluxes and flavors (since no hadronic processes involved) when the muon polarization is known;
- flexibility in the choice of the beam energy, since precisely determined by the muon storage ring energy.

These beams will contain neutrinos of the electron and muon flavors in same quantity, i.e.  $\mu^- \rightarrow e^- \nu_\mu \bar{\nu}_e$  or  $\mu^+ \rightarrow e^+ \nu_e \bar{\nu}_\mu$ , a feature that distinguishes them from traditional neutrino beams where  $\nu_\mu$  dominates (since  $\pi \rightarrow e \nu_e$  is suppressed).

This well-defined flavor composition can be exploited using a detector with charge identification capabilities to search for neutrino oscillations. In Ref. [1], we have studied a possible  $\nu_\mu \rightarrow \nu_e$  oscillation search to study the LSND claim with a detector placed at a medium baseline.

Perhaps the most interesting option is the fact that muon beams will be located next to muon colliders which necessarily require very intense proton sources. This opens the possibility to obtain very intense neutrino beams to perform long and very long baseline oscillation experiments.

In Ref. [2], we have considered a  $\nu_\mu$  disappearance experiment with a baseline of 730 km. Since the neutrino beams contain both electron and muon flavors, the disappearance of muon neutrino can be performed by directly comparing electron and muon events. This method is self normalizing, i.e. without the need of a near detector to predict the original flux.

Therefore, the very attractive feature for the future, rather than to think of experiments on currently accessible baselines (i.e. the FNAL-NUMI to Soudan and the CERN-NGS to GranSasso) is to imagine a second generation of long baseline experiments with very long baseline of the order of 6500-8800 km, made possible by the intense neutrino sources.

## 2 Oscillation searches at VLBL

The distance  $L$  between neutrino production and detection is a key element in oscillation studies. Since the oscillation probability varies like

$$\sin^2(1.27\Delta m^2(eV^2)L(km)/E_\nu(GeV)),$$

having a longer length means the possibility to explore the same parameter-space region with neutrinos of higher energy.

In addition, since these beams will travel through Earth for thousands of kilometers, matter enhancement in neutrino oscillation [3] can become important, as recently pointed out in Ref. [4]. We perform oscillation searches that can be categorized as follows:

- **$\mu$  disappearance:** similar to what we described in Ref. [2]; but improved due to the larger  $L/E$  ratio, to observe the “dip” in the  $\nu_\mu$  energy distribution, even for the lowest  $\Delta m^2$  suggested by the atmospheric neutrino effect.
- **$e$  and  $\mu$  appearances:** study of matter effects in  $\nu_e \rightarrow \nu_\mu$  oscillations  
Travel through the Earth would enhance the transition probability for neutrinos (antineutrinos) if  $\Delta m^2 > 0$  ( $\Delta m^2 < 0$ ). Running the muon storage ring alternatively with negative and positive muons would directly reveal this effect and determine the sign of  $\Delta m^2$ .
- **$\tau$  appearance:** the production of  $\tau$  leptons can be determined looking for an excess of hadronic events due to hadronic  $\tau$  decays.

We do not consider the possibility of direct tau appearance by identification of the  $\tau$  lepton using kinematical or topological criteria, and postpone it to further studies.

## 3 Possible very long baselines

We assume that a multikiloton detector will be located in Europe at the Laboratori Nazionali del GranSasso (LNGS, Italy).

The ideal detector would be a 10 kiloton (fiducial) SuperICARUS as described in Ref. [5]. In addition to providing excellent spatial resolution like that of bubble-chamber, SuperICARUS, unlike most neutrino detectors, allows for excellent electron identification and measurement. High energy muons, exiting the detector, can also be measured from multiple scattering with a resolution  $\Delta p/p \approx 20\%$ . These unique lepton capabilities are in a sense matched to the beams from muon decays, which provide equal amounts of electron and muon neutrinos.

We also assume that a “sign-determining” muon spectrometer is installed behind the target, to allow the identification of the leading muon charge (“ $\mu^-$ ”, “ $\mu^+$ ” samples). On the other hand, the leading electron charge cannot be identified (“ $e^-$ ” sample). This is due to the fact that electrons will produce a shower soon after production before being sufficiently bent in a possible magnetic field to be measured.

The neutrino source could be located in different laboratories around the world, in the American or Asian continent. For example, we quote BNL-GranSasso, FNAL-GranSasso and KEK-GranSasso. The BNL-LNGS has a baseline of  $L = 6500$  km (see Figure 1). The beam goes to a maximum depth of 900 km and arrives at GS with an angle with respect to horizontal of about  $30^\circ$ . We estimate the average density of the Earth[7] for this baseline to be  $\rho = 3.6$  g/cm<sup>3</sup>. Other baselines are FNAL-GranSasso ( $L = 7400$  km, max. depth 1200 km, average density  $\rho = 3.7$  g/cm<sup>3</sup>, beam angle  $36^\circ$ ) or KEK-GranSasso ( $L = 8800$  km, max. depth 1800 km, average density  $\rho = 4.0$  g/cm<sup>3</sup>, beam angle  $44^\circ$ ). There is not much differences in  $L$  between the various baselines.

Our attention was recently drawn to the upgrade of the AGS accelerator in BNL[6]. A total of  $6.6 \times 10^{21}$  protons on target per year could be produced. When used as proton driver

of a muon accumulator with a muon yield per proton of 15%, we obtain  $6.6 \times 10^{21} \times 0.15 = 9.9 \times 10^{20}$  muons/year. The machine would be operated for four years, alternating runs with positive and negative muons and we consider that, given the shape of the muon storage ring, half of the muons will decay in the direction towards the GranSasso laboratory. We then use as integrated intensity a total of

$$N(\mu^+) + N(\mu^-) = \frac{1}{2} \times 6.6 \times 10^{21} \times 0.15 \times 4 \approx 2 \times 10^{21} \mu's$$

decay in the right direction producing neutrinos.

## 4 Event rates for the BNL/AGS-GS baseline

Neutrinos travel the distance between the BNL and GS laboratories and are then detected in the 10 kton (fiducial) detector.

The neutrino event rate will grow as  $E_\mu^3$  where  $E_\mu$  is the energy of the muon storage ring. We are interested in a neutrino beam with energy of about 20 GeV. We list in Table 1 the neutrino event rates in case of no oscillation as a function of the muon storage ring energy, for  $10^{21}$  muons decays of a given charge and 10 kton target. Neutrino interactions have been divided into charged current (CC) and neutral current (NC) interactions. The CC events are split into inelastic scattering (DIS) and quasi-elastic (QE) interactions.

$E_\mu$ (GeV)	$10^{21} \mu^-$ decays			$10^{21} \mu^+$ decays		
	CC( $\bar{\nu}_e$ )	CC( $\nu_\mu$ )	NC	CC( $\nu_e$ )	CC( $\bar{\nu}_\mu$ )	NC
10	426	1152	196	1016	488	173
15	1414	3751	1129	3283	1624	1005
20	3313	8712	3542	7588	3820	3172
25	6412	16746	8221	14568	7401	7419
30	11010	28576	16008	24850	12710	14524

Table 1: The total number of neutrinos detected in a 10 kton (fiducial) detector for a baseline  $L = 6500$  km and a total number of  $10^{21}$  muons decays.

## 5 Neutrino oscillation scenarios

In the preceding section, we have seen that the expected neutrino event rates are comfortable and open possibilities to study various neutrino oscillations scenarios with a baseline of

$$\frac{E}{L} \approx \frac{20 \text{ GeV}}{6500 \text{ km}} \approx 2.5 \times 10^{-3} \text{ eV}^2.$$

While the atmospheric neutrino evidence is compatible with maximal mixing between  $\nu_\mu$  and  $\nu_\tau$ , it is attractive to think that there is also a smaller mixing between the first and third family. We therefore consider a three-family scenario. The mixing between the different neutrino flavors is determined by two mass differences and a unitary matrix describing the mixing between flavor and mass eigenstates.

We base our computation on the formalism of Ref. [4] and make the approximation that only a mass scale is relevant, i.e. assuming that the differences  $|m_3^2 - m_2^2| \gg |m_2^2 - m_1^2|$  (this approximation being supported by current experimental results on solar neutrinos). The

mass eigenstate  $m_1$  is defined orthogonal to the electron flavor state. The mixing matrix takes a form that only depends on the two mixing angles  $\theta$  and  $\phi$ :

$$U = \begin{pmatrix} 0 & \cos \theta & \sin \theta \\ \cos \phi & -\sin \theta \sin \phi & \cos \theta \sin \phi \\ -\sin \phi & -\sin \theta \cos \phi & \cos \theta \cos \phi \end{pmatrix} \quad (1)$$

The three-family oscillation is therefore described by only three parameters: the mass difference between the second and third neutrino  $\Delta m^2 \equiv \Delta m_{23}^2$  and the two mixing angles  $\theta$  and  $\phi$ .

The long travel inside the Earth gives rise to matter effects, resulting in a modification of the oscillation. The mixing angle in matter  $\theta_m$  takes a value given by the expression

$$\sin^2 2\theta_m(x) = \frac{\sin^2 2\theta}{\sin^2 2\theta + (x - \cos 2\theta)^2}$$

and

$$x = \frac{2VE_\nu}{\Delta m^2} = \pm \frac{2\sqrt{2}G_F n_e E_\nu}{\Delta m^2},$$

where the plus sign applies to  $\nu$ 's and the minus to  $\bar{\nu}$ 's and  $n_e$  is the electron density of the medium. In the limit of no matter effects  $x \rightarrow 0$  and the mixing angle  $\theta_m \rightarrow \theta$ . Given the distance between the two laboratories, the beam reaches the maximal depth of about 900 km, where the matter density of the earth is larger than that close to the surface (we derive this information from Ref. [7]). An average matter density of  $3.6 \text{ g/cm}^3$  was considered.

## 6 Oscillated neutrino fluxes

We assume that the mixing is maximal between the second and the third neutrino family ( $\sin^2 \phi = 0.5$ ) and small ( $\sin^2 \theta = 0.025$ ) between the first two. We will consider the three values of  $\Delta m^2 = 10^{-3}, 3 \times 10^{-3}$  and  $10^{-2} \text{ eV}^2$ .

In the case of a neutrino beam from negative muons, four oscillation processes will occur:

- $\nu_\mu \rightarrow \nu_e$
- $\nu_\mu \rightarrow \nu_\tau$
- $\bar{\nu}_e \rightarrow \bar{\nu}_\mu$
- $\bar{\nu}_e \rightarrow \bar{\nu}_\tau$

while for the case of positive muons the charge-conjugate processes occur.

The neutrino fluxes as a function of energy for the different flavors in the case of three-family oscillations are shown in Figure 2 for a 30 GeV muon beam and  $\Delta m^2 = 3 \times 10^{-3} \text{ eV}^2$ .

## 7 Event classification

We classify the observed events in four classes:

- a) events with electrons or positrons (no electron charge measured),
- b) events with muons of the same sign of those circulating in the storage ring,
- c) events with muons of opposite sign,
- d) events without leptons.

No direct  $\tau$  identification is performed, so, according to their decay,  $\tau$  events are seen either in the electron ( $\tau \rightarrow e$  decays), muon ( $\tau \rightarrow \mu$ ) or neutral current ( $\tau \rightarrow h$ ) sample.

Figure 3 shows the energy spectra of the four classes for a 30 GeV  $\mu^-$  beam. The dotted and full lines refer to the predicted distributions without oscillations, and with oscillations with  $\Delta m^2 = 3 \times 10^{-3} eV^2$ . In Figure 4 the same distributions are shown for 30 GeV  $\mu^+$  beams.

Let us consider in more detail the processes playing a role for the different classes of observed events. In the following, every process is listed with the relevant probability, where the notation  $P_{\nu_\alpha \rightarrow \nu_\beta}$  is used to identify the probability of neutrinos of flavor  $\alpha$  to oscillate into neutrinos of flavor  $\beta$ . These probabilities (and the text, unless otherwise specified) refer to the case of negative muons in the storage ring; the charge-conjugate must be considered for the case of positive muons.

## 7.1 Events with electrons

In these events, a leading electron or positron is identified in the detector. Such events could be produced by the charged-current interactions of the following neutrinos:

1. unoscillated  $\bar{\nu}_e$  neutrinos from the beam  
 $(1 - P_{\bar{\nu}_e \rightarrow \bar{\nu}_\mu} - P_{\bar{\nu}_e \rightarrow \bar{\nu}_\tau}) \times \Phi_{\bar{\nu}_e}$
2. muon neutrinos oscillated into electron neutrinos  
 $(P_{\nu_\mu \rightarrow \nu_e}) \times \Phi_{\nu_\mu}$
3. tau neutrinos derived from oscillations followed by a  $\tau \rightarrow e$  decay  
 $(P_{\nu_\mu \rightarrow \nu_\tau} \times BR(\tau^- \rightarrow e))\Phi_{\nu_\mu} + (P_{\bar{\nu}_e \rightarrow \bar{\nu}_\tau} \times BR(\tau^+ \rightarrow e))\Phi_{\bar{\nu}_e}$

In case of  $\mu^-$  beams, process 1) will deplete the number of leading electron events from the beam, while process 2) will increase the number of such events, as they come from oscillation of muon neutrinos. Since process 2) involves neutrinos, it is matter-enhanced, and the net effect will be an increase of the number of observed events having a leading electron with respect to the case of no oscillation, as can be seen comparing the Figures in Table 2 with the non-oscillated case (Table 1).

In the case of  $\mu^+$  beams, the balance of the two competing processes is reversed. Now process 1) involves neutrinos, so the depletion of electron events from the beam is matter-enhanced, while process 2) is suppressed. The net effect is a smaller number of observed events with leading electrons with respect to the expectations, as can be seen comparing Tables 3 and 1.

$E_\mu$ (GeV)	$\Delta m^2 (eV^2)$	unoscillated beam $(1 - P_{\bar{\nu}_e \rightarrow \bar{\nu}_\mu}) \times \Phi_{\bar{\nu}_e}$	$\nu_\mu \rightarrow \nu_e$ $(P_{\nu_\mu \rightarrow \nu_e}) \times \Phi_{\nu_\mu}$	$\tau$ decay $((P_{\nu_\mu \rightarrow \nu_\tau})\Phi_{\nu_\mu} + (P_{\bar{\nu}_e \rightarrow \bar{\nu}_\tau})\Phi_{\bar{\nu}_e})$ $\times BR(\tau \rightarrow e)$
10	$1. \times 10^{-3}$	424.	56.	17
20		3309.	76.	118
30		11011.	85.	271
10	$3. \times 10^{-3}$	418	252	6
20		3268	977	380
30		10967	1366	1423
10	$1. \times 10^{-2}$	411	40	11
20		3213	449	314
30		10820	5805	574

Table 2: Different contributions to leading electron events from  $\mu^-$  beams.

$E_\mu$ (GeV)	$\Delta m^2(eV^2)$	unoscillated beam $(1 - P_{\nu_e \rightarrow \nu_x}) \times \Phi_{\nu_e}$	$\bar{\nu}_\mu \rightarrow \bar{\nu}_e$ $(P_{\bar{\nu}_\mu \rightarrow \bar{\nu}_e}) \times \Phi_{\bar{\nu}_\mu}$	$\tau$ decay $((P_{\bar{\nu}_\mu \rightarrow \bar{\nu}_\tau})\Phi_{\bar{\nu}_\mu} + (P_{\nu_e \rightarrow \nu_\tau})\Phi_{\nu_e})$ $\times BR(\tau \rightarrow e)$
10 20 30	$1. \times 10^{-3}$	874. 7377. 24624.	1. 1. 3.	10 58 128
10 20 30	$3. \times 10^{-3}$	644 5413 21457	5 17 15	7 233 761
10 20 30	$1. \times 10^{-2}$	941 6929 17208	10 45 120	6 161 521

Table 3: Different contributions to leading electron events from  $\mu^+$  beams.

### 7.1.1 Quasi-elastic events

The electron charge is not measured. In order to identify neutrino or antineutrino interactions without the need of a measurement of the electron charge, quasi-elastic interactions can however be used. In particular,

$$\nu_e + n \rightarrow e^- + p$$

events are quite cleanly distinguishable from DIS processes, due to the presence of a proton, seen in the detector as a highly ionizing track. The same does not hold for antineutrino interactions

$$\bar{\nu}_e + p \rightarrow e^+ + n$$

since the neutrons do not produce any track at the vertex.

The presence of  $e + p$  final state in a beam from  $\mu^-$  is therefore a clear signature for  $\nu_\mu \rightarrow \nu_e$  oscillation. The total rate of  $e^-p$  events produced in quasi-elastic interactions from a beam of negative muons is listed in Table 4. The number of quasi-elastic events is non negligible, even after taking into account the detection efficiency due to a necessary proton momentum threshold for detection and rejection of nuclear spectators protons.

$E_\mu$ (GeV)	$\Delta m^2(eV^2)$	$e^-p$ events (QE) $(P_{\nu_\mu \rightarrow \nu_e}) \times \Phi_{\nu_\mu}$	$e^+n$ events (QE) $(1 - P_{\bar{\nu}_e \rightarrow \bar{\nu}_x}) \times \Phi_{\bar{\nu}_e}$
10 20 30	$1. \times 10^{-3}$	7 7 6	58 258 598
10 20 30	$3. \times 10^{-3}$	21 55 61	57 254 595
10 20 30	$1. \times 10^{-2}$	4 21 169	56 250 587

Table 4: Number of quasi-elastic interactions ( $e^-p$  final states) from neutrinos produced in  $\mu^-$  beams

## 7.2 Events with right-sign muons

The muon charge is measured by a spectrometer placed behind the detector. Muons of the same sign of those decaying in the storage ring are produced by:

1. muon neutrinos coming from the beam  
 $(1 - P_{\nu_\mu \rightarrow \nu_e} - P_{\nu_\mu \rightarrow \nu_\tau}) \times \Phi_{\nu_\mu}$
2.  $\tau$  decays, where the  $\tau$  is coming from  $\nu_\mu \rightarrow \nu_\tau$  or  $\bar{\nu}_e \rightarrow \bar{\nu}_\tau$  oscillations.  
 $P_{\nu_\mu \rightarrow \nu_\tau} \times BR(\tau \rightarrow \mu) \times \Phi_{\nu_\mu}$

Since in this case we measure the muon sign,  $\nu_\mu$  oscillating into  $\nu_e$  are not compensated by  $\bar{\nu}_e$  oscillations into  $\bar{\nu}_\mu$ , as they produce muons of opposite charge (see following subsection). A small compensation to the total number of right-sign muons comes from  $\nu_\mu \rightarrow \nu_\tau$  oscillations where the  $\tau$  decays into a muon. For both  $\mu^-$  and  $\mu^+$  events, the net effect of neutrino oscillations is a disappearance of right-sign leading muon events.

## 7.3 Events with wrong-sign muons

Opposite-sign muons can only be produced by neutrino oscillations, since there is no component in the beam that could account for them. These events are coming from oscillations of the electron component of the beam:

1. directly via  $\bar{\nu}_e \rightarrow \bar{\nu}_\mu$  oscillations  
 $P_{\bar{\nu}_e \rightarrow \bar{\nu}_\mu} \times \Phi_{\bar{\nu}_e}$
2. via  $\tau$  decays after  $\bar{\nu}_e \rightarrow \bar{\nu}_\tau$  oscillations.  
 $P_{\bar{\nu}_e \rightarrow \bar{\nu}_\tau} \times BR(\tau \rightarrow \mu) \times \Phi_{\bar{\nu}_e}$

Opposite sign muons could be produced in decays of hadrons in neutral current events. We note however that these muons will be soft and not isolated from the jet and can therefore be suppressed by a mild isolation and momentum cut.

For reasons opposite to those already explained in the discussion of events with leading electrons, the production of events opposite-sign muons is suppressed in beams from  $\mu^-$  decays, and enhanced in beams from  $\mu^+$  decays. Since this enhancement is due to the presence of matter, the energy spectrum of these events has a peak close to the resonance energy (about 11 GeV for  $\Delta m^2 = 3 \times 10^{-3} eV^2$ ).

The number of events for both same-sign and wrong-sign muons are shown in Tables 5 and 6.

$E_\mu$ (GeV)	$\Delta m^2 (eV^2)$	$\bar{\nu}_e \rightarrow \bar{\nu}_\mu$ $\mu^+$	$\bar{\nu}_e \rightarrow \bar{\nu}_\tau$ $\mu^+$	unoscillated beam $\mu^-$	$\nu_\mu \rightarrow \nu_\tau$ $\mu^-$
10.	$1. \times 10^{-3}$	1.	0.	315.	17
20.		1.	0.	6096.	115
30.		3.	0.	24342.	265
10.	$3. \times 10^{-3}$	4	0	580	6
20.		22	1	1049	370
30.		24	1	7893	1390
10.	$1. \times 10^{-2}$	8	0	614	11
20.		49	2	2784	305
30.		98	6	14200	555

Table 5: Different contributions to leading-muon events from  $\mu^-$  beams

$E_\mu$ (GeV)	$\Delta m^2 (eV^2)$	$\nu_e \rightarrow \nu_\mu$ $\mu^-$	$\nu_e \rightarrow \nu_\tau$ $\mu^-$	unoscillated beam $\mu^+$	$\bar{\nu}_\mu \rightarrow \bar{\nu}_\tau$ $\mu^+$
10.	$1. \times 10^{-3}$	71.	1.	133.	9
20.		104.	3.	2667.	54
30.		120.	5.	10824.	120
10.	$3. \times 10^{-3}$	186	4	349	3
20.		1086	44	562	183
30.		1703	90	3484	655
10.	$1. \times 10^{-2}$	38	1	260	5
20.		328	15	1268	142
30.		3828	282	9045	227

Table 6: Different contributions to leading-muon events from  $\mu^+$  beams

#### 7.4 Events with no leading leptons

Events with no leading leptons can be produced in

1. neutral current processes
2. hadronic  $\tau$  decays

$$P_{\nu_\mu \rightarrow \nu_\tau} \times BR(\tau \rightarrow \text{hadrons}) \times \Phi_{\nu_\mu} + P_{\bar{\nu}_e \rightarrow \bar{\nu}_\tau} \times BR(\tau \rightarrow \text{hadrons}) \times \Phi_{\bar{\nu}_e}$$

The neutral current processes do not depend on the oscillations, so there is always an excess of events in this class, due to the hadronic  $\tau$  decays, with respect to the expectation.

Total number of events for these two categories is shown in Table 7, for both  $\mu^-$  and  $\mu^+$  beams.

$E_\mu$ (GeV)	$\Delta m^2 (eV^2)$	$\mu^-$ beam		$\mu^+$ beam	
		NC	$\tau \rightarrow \text{hadrons}$	NC	$\tau \rightarrow \text{hadrons}$
10.	$1. \times 10^{-3}$	196.	62	173.	35
20.		3534.	429	3168.	213
30.		16061.	986	14553.	466
10.	$3. \times 10^{-3}$	196	21	173	25
20.		3534	1383	3168	847
30.		16061	5180	14553	2771
10.	$1. \times 10^{-2}$	196	40	173	23
20.		3534	1143	3168	585
30.		16061	2091	14553	1896

Table 7: Different contributions to events with no leading leptons.

## 8 Ratios of observed versus expected events

Given the large oscillation probabilities, the oscillation signatures will appear strongly. We illustrate this by computing the ratios of observed over expected events for the four classes. These numbers are shown in Tables 8 and 9 with their statistical error. In all cases, the effect is significant; to increase further the electron case, it is possible to take the double ratio between events detected with negative and positive muons.



$E_\mu$ (GeV)	$\Delta m^2$ (eV <sup>2</sup> )	$\nu_e + \bar{\nu}_e/\bar{\nu}_e^{EXP.}$	$\nu_\mu/\nu_\mu^{EXP.}$	$\bar{\nu}_\mu/\nu_\mu^{EXP.}$	$NC/NC^{EXP}$
10.0	$1. \times 10^{-3}$	$1.167 \pm 0.052$	$0.288 \pm 0.0158$	$0.0008 \pm 0.0008$	$1.318 \pm 0.082$
20.0		$1.058 \pm 0.018$	$0.714 \pm 0.0091$	$0.0001 \pm 0.0001$	$1.122 \pm 0.018$
30.0		$1.032 \pm 0.010$	$0.859 \pm 0.0055$	$0.0001 \pm 0.0001$	$1.061 \pm 0.008$
10.0	$3. \times 10^{-3}$	$1.586 \pm 0.061$	$0.508 \pm 0.0210$	$0.0036 \pm 0.0018$	$1.107 \pm 0.075$
20.0		$1.397 \pm 0.021$	$0.163 \pm 0.0043$	$0.0026 \pm 0.0005$	$1.391 \pm 0.020$
30.0		$1.249 \pm 0.011$	$0.324 \pm 0.0034$	$0.0009 \pm 0.0002$	$1.323 \pm 0.009$
10.0	$1. \times 10^{-2}$	$1.083 \pm 0.050$	$0.542 \pm 0.0217$	$0.0067 \pm 0.0024$	$1.203 \pm 0.078$
20.0		$1.201 \pm 0.019$	$0.355 \pm 0.0064$	$0.0059 \pm 0.0008$	$1.324 \pm 0.019$
30.0		$1.561 \pm 0.012$	$0.515 \pm 0.0042$	$0.0036 \pm 0.0004$	$1.130 \pm 0.008$

Table 8: Ratio between the events observed in each class for negative muon decays, and the events that would be observed without oscillation. Errors are statistical only

$E_\mu$ (GeV)	$\Delta m^2$ (eV <sup>2</sup> )	$\nu_e + \bar{\nu}_e/\nu_e^{EXP.}$	$\nu_\mu/\bar{\nu}_\mu^{EXP.}$	$\bar{\nu}_\mu/\bar{\nu}_\mu^{EXP.}$	$NC/NC^{EXP}$
10.0	$1. \times 10^{-3}$	$0.870 \pm 0.029$	$0.290 \pm 0.0244$	$0.1467 \pm 0.0173$	$1.202 \pm 0.083$
20.0		$0.980 \pm 0.011$	$0.714 \pm 0.0137$	$0.0281 \pm 0.0027$	$1.202 \pm 0.018$
30.0		$0.996 \pm 0.006$	$0.858 \pm 0.0082$	$0.0098 \pm 0.0009$	$1.032 \pm 0.008$
10.0	$3. \times 10^{-3}$	$0.646 \pm 0.025$	$0.720 \pm 0.0384$	$0.3890 \pm 0.0282$	$1.146 \pm 0.081$
20.0		$0.747 \pm 0.010$	$0.196 \pm 0.0072$	$0.2965 \pm 0.0088$	$1.267 \pm 0.020$
30.0		$0.894 \pm 0.006$	$0.325 \pm 0.0050$	$0.1406 \pm 0.0033$	$1.190 \pm 0.009$
10.0	$1. \times 10^{-2}$	$0.941 \pm 0.030$	$0.543 \pm 0.0333$	$0.0787 \pm 0.0127$	$1.131 \pm 0.081$
20.0		$0.941 \pm 0.011$	$0.370 \pm 0.0099$	$0.0900 \pm 0.0049$	$1.185 \pm 0.019$
30.0		$0.718 \pm 0.005$	$0.727 \pm 0.0076$	$0.3324 \pm 0.0050$	$1.130 \pm 0.009$

Table 9: Same as previous Table, but for the decay of positive muons.

In order to measure the oscillation parameters, it is interesting to notice the dependence on  $\Delta m^2$  of the energy spectrum of wrong-sign muons. The position of the peak of the distribution depends on the resonance energy, which is a function of  $\Delta m^2$ . In Figure 5 this distribution is shown for  $\Delta m^2$  values of  $1, 2, 3, 4 \times 10^{-3}$  eV<sup>2</sup>.

## 9 Interpretation of experimental results

A fit to the observed energy distributions and rates allows the determination of the parameters  $\Delta m^2$ ,  $\theta$  and  $\phi$  governing the oscillation; the fit probability is a test of the hypothesis that one mass scale is relevant, and that there are no other processes or phenomena (i.e. sterile neutrinos). Given the statistical accuracies obtained in Tables 8 and 9, we foresee that these fits will give good constraints on the oscillation parameters and scenarios.

## 10 Conclusions

The possibility of performing a second generation very-long baseline experiment using an intense neutrino beam from negative and positive muons offers the unique opportunity to study the  $\Delta m^2$  region indicated by the atmospheric neutrinos. At the chosen optimized  $L/E$  distance, the oscillation probabilities are maximized and will allow a complete understanding of the oscillation parameters governing the  $\nu_\mu \rightarrow \nu_\tau$  oscillation. Even in the case where a simple counting experiment is performed like the one we have assumed, the visible effects are

significant. A large disappearance of muon neutrinos not compensated by the appearance of taus — e.g.  $\nu_\mu \rightarrow \nu_s$  — would be immediately noticed. In addition, the unique feature of the muon decay beams providing electron and muon neutrinos in same quantities, allow the study matter effects in Earth and given the distance and energies involved should reveal directly the presence of the oscillation resonance. By a change of sign in the muon storage ring, the matter effects can be studied by directly comparing the oscillations of neutrinos and their anti-neutrinos.

## Acknowledgments

We are indebted to R. Palmer for enlighting us on the possible upgrade of the AGS at BNL.

## References

- [1] A.Bueno, M.Campanelli, A.Rubbia “A medium baseline search for  $\nu_\mu \rightarrow \nu_e$  oscillations at a  $\nu$  beam from muon decays” hep-ph/9809252 CERN-EP/98-140 accepted by IJMP.
- [2] A.Bueno, M.Campanelli, A.Rubbia “Long baseline neutrino oscillation disappearance search using a  $\nu$  beam from muon decays” hep-ph/9808485 ETHZ-IPP-98-05 accepted by IJMP.
- [3] L. Wolfenstein, Phys. Rev. **D17**, 2369 (1978); Phys. Rev. **D 20**, 2634 (1979); Mikheyev and Smirnov, Sov.J.Nucl.Phys. **42**, 913 (1986).
- [4] P.Lipari, hep-ph/9903481.
- [5] ICARUS collaboration, “*ICARUS-Like Technology for Long Baseline Neutrino Oscillations*”, CERN/SPSC/98-33 & M620, 1998 and references therein.
- [6] Robert Palmer and Thomas Roser, private communications.
- [7] J. Bahcall, P. Krastev, Phys. Rev. **C56** 2839-2857, 1997.

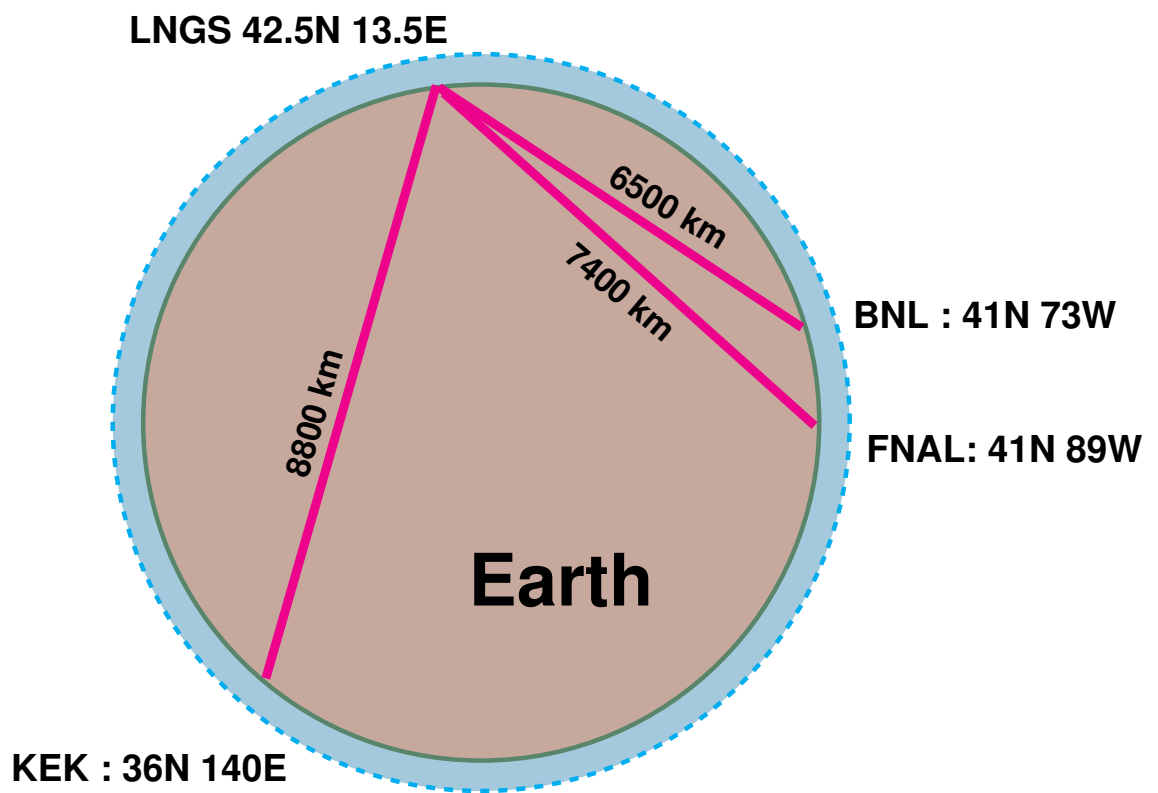


Figure 1: Possible very long baselines across the Earth (seen from above the North pole).

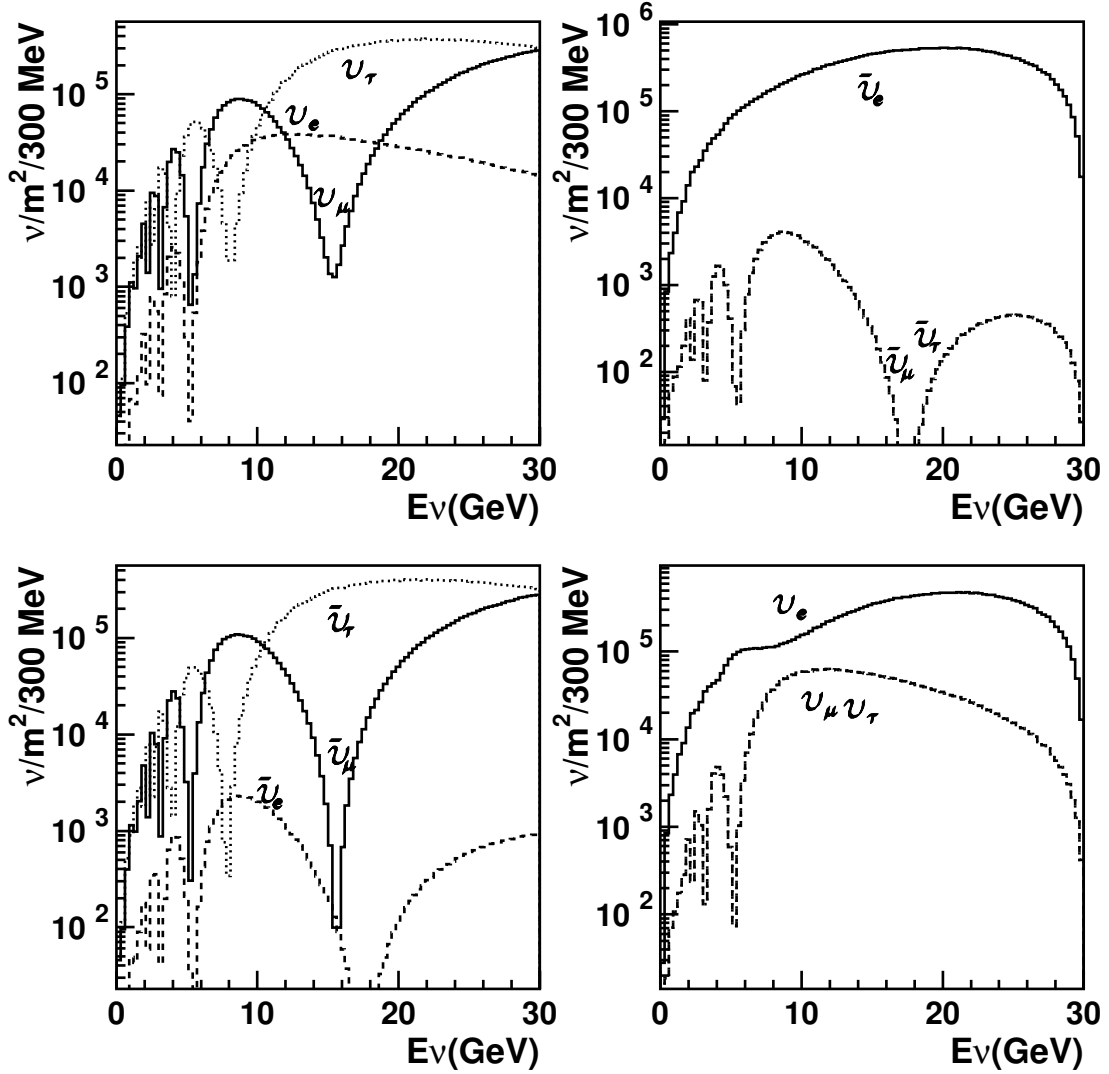


Figure 2: The oscillated neutrino fluxes reaching the detector per  $m^2$  normalized to  $10^{21}$  muon decays. The oscillation probability is given for three-family mixing with  $\Delta m^2 = 3 \times 10^{-3} eV^2$ ,  $\sin^2 \phi = 0.5$ ,  $\sin^2 \theta = 0.025$ . The two upper plots refer to decays of  $30 \text{ GeV } \mu^-$ , the two lower to decays of  $\mu^+$ . The matter enhancement (suppression) is clearly visible for the  $\nu_e$  ( $\bar{\nu}_e$ ) cases. The  $\nu_\mu$  ( $\bar{\nu}_\mu$ ) fluxes are largely suppressed with a spectacular “hole” in the spectrum due to maximal oscillation to  $\nu_\tau$ . The  $\nu_e \rightarrow \nu_\mu$  and  $\nu_e \rightarrow \nu_\tau$  ( $\bar{\nu}_e \rightarrow \bar{\nu}_\mu$  and  $\bar{\nu}_e \rightarrow \bar{\nu}_\tau$ ) contributions are also visible.

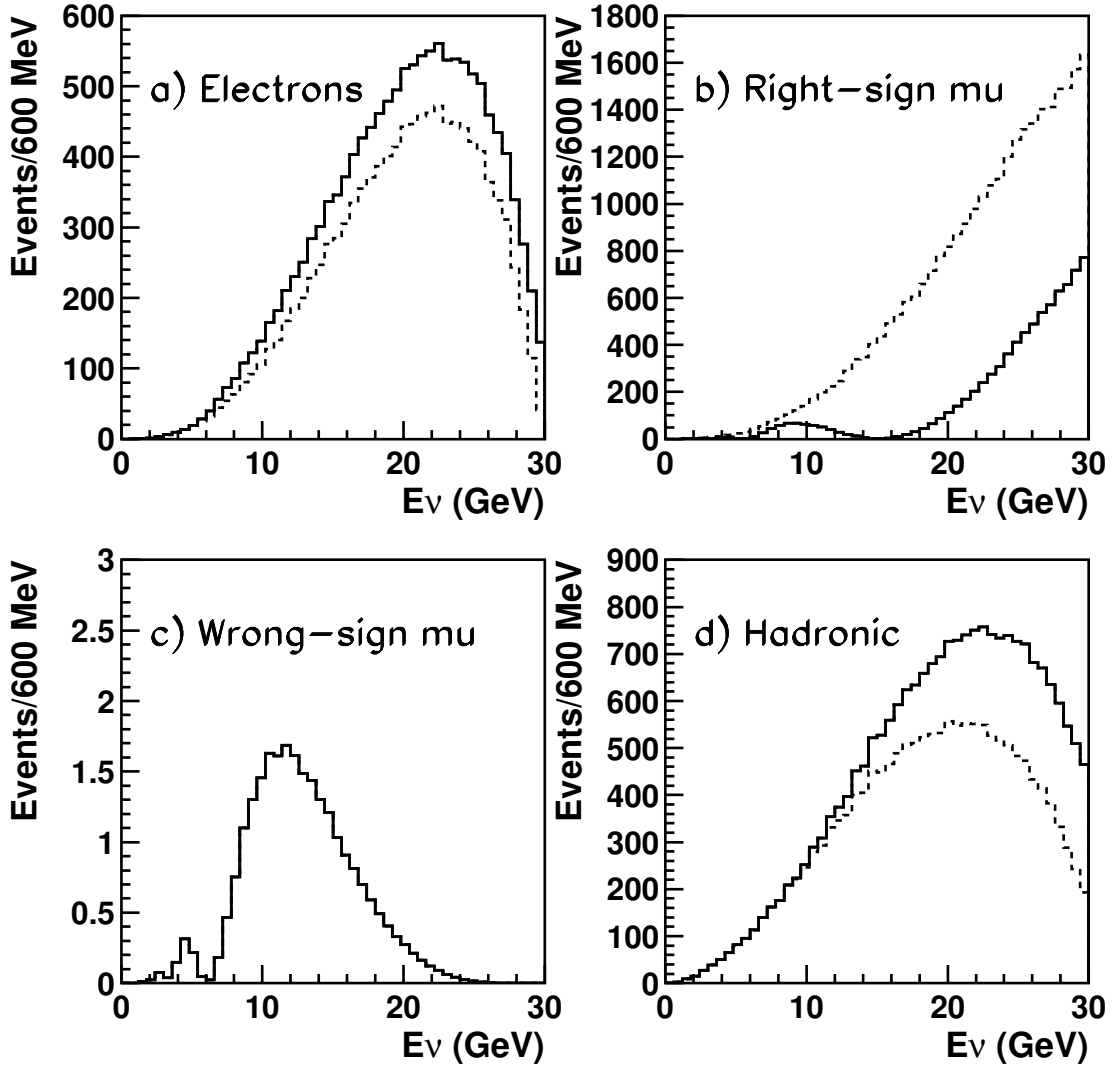


Figure 3: Predicted event energy spectrum of the four classes of events a) with leading electron or positron, b) with leading right-sign muons, c) with leading opposite sign muons d) events with no leading leptons. Full line: spectra with oscillations; dashed line: spectra without oscillations. The plots are for  $10^{21} \mu^-$  decays. The muon energy is 30 GeV and the target mass is 10 kton. The spectacular disappearance of right-sign muon is visible in plot b). The suppression due to matter effects is clearly visible in plot c) which contain the opposite-sign muon events. The appearance of tau can be directly observed as an excess of neutral current like events (plot d).

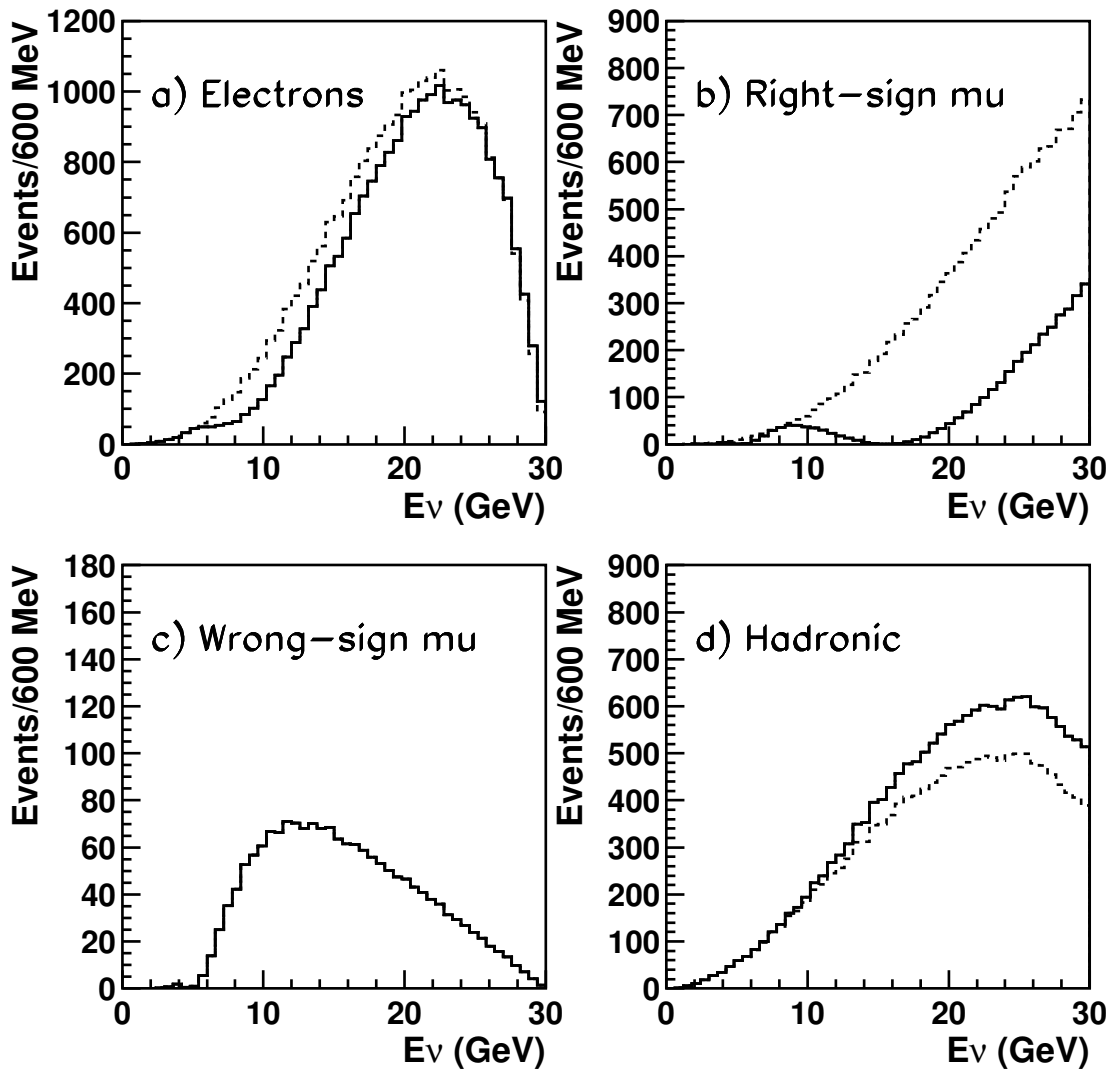


Figure 4: Same as previous plot, but 30 GeV  $\mu^+$  decays. The sign of the muon charges are also exchanged, i.e. plot b refers to events with leading  $\mu^+$ , plot c to events with leading  $\mu^-$ . In this case, the enhancement due to matter effects is clearly visible.

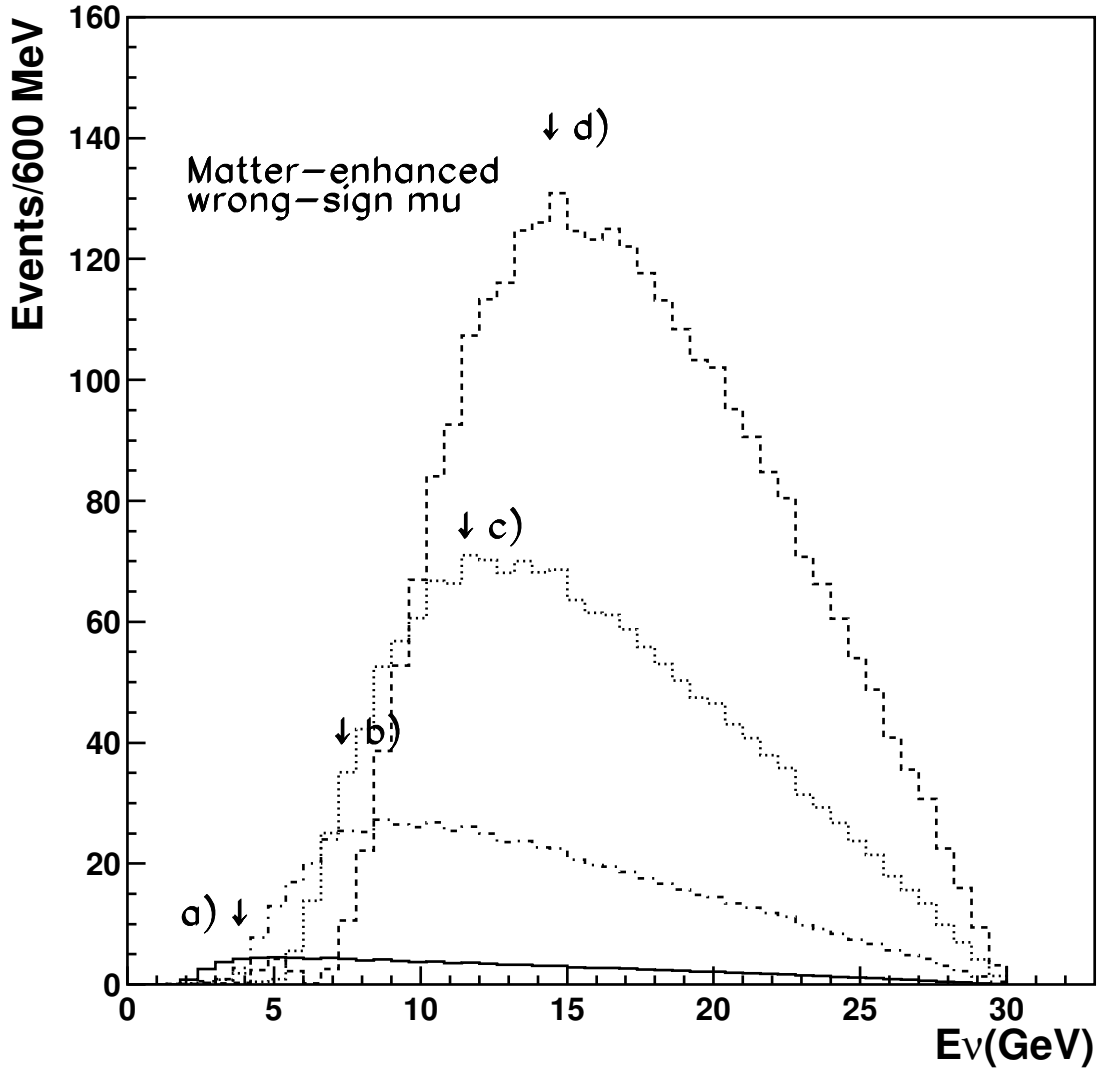


Figure 5: Energy spectra of events with leading  $\mu^-$  in a decay beam of positive muons. The different distributions refer to the following values of  $\Delta m^2(eV^2)$ : a)  $1 \times 10^{-3}$ , b)  $2 \times 10^{-3}$ , c)  $3 \times 10^{-3}$ , d)  $4 \times 10^{-3}$ . The shift in the peak position, corresponding to the resonance of oscillations due to matter effects (indicated by an arrow) is clearly visible.

# Three-family oscillations using neutrinos from muon beams at very long baseline

M. Campanelli<sup>1</sup>, A. Bueno<sup>1</sup>, A. Rubbia<sup>1,2</sup>

<sup>1</sup> *Institut für Teilchenphysik, ETHZ, CH-8093 Zürich, Switzerland*

<sup>2</sup> *CERN, CH-1211 Geneva 23, Switzerland*

## Abstract

The planned LBL experiments will be able to prove the hypothesis of flavor oscillation between muon and tau neutrinos. We explore the possibility of a second generation long baseline experiment at very long baseline, i.e.  $L$  in the range 5000 – 7000 km. This distance requires intense neutrino beams that could be available from very intense muon beams as those needed for  $\mu$  colliders. Such baselines allow the study of neutrino oscillations with  $E/L \approx 2 \times 10^{-3} \text{ eV}^2$  with neutrinos of energy  $E_\nu \approx 10 \text{ GeV}$ , i.e. above tau threshold. Moreover, matter effects inside the Earth could lead to observable effects in  $\nu_e \rightarrow \nu_\mu$  oscillations. These effects are interchanged between neutrinos and antineutrinos, and therefore they can be tested by comparing the oscillated spectra obtained running the storage ring with positive and negative muons.

## 1 Introduction

The use of neutrinos from muon decays has several advantages:

- easy prediction of the neutrino fluxes and flavors (since no hadronic processes involved) when the muon polarization is known;
- flexibility in the choice of the beam energy, since precisely determined by the muon storage ring energy.

These beams will contain neutrinos of the electron and muon flavors in same quantity, i.e.  $\mu^- \rightarrow e^- \nu_\mu \bar{\nu}_e$  or  $\mu^+ \rightarrow e^+ \nu_e \bar{\nu}_\mu$ , a feature that distinguishes them from traditional neutrino beams where  $\nu_\mu$  dominates (since  $\pi \rightarrow e \nu_e$  is suppressed).

This well-defined flavor composition can be exploited using a detector with charge identification capabilities to search for neutrino oscillations. In Ref. [1], we have studied a possible  $\nu_\mu \rightarrow \nu_e$  oscillation search to study the LSND claim with a detector placed at a medium baseline.

Perhaps the most interesting option is the fact that muon beams will be located next to muon colliders which necessarily require very intense proton sources. This opens the possibility to obtain very intense neutrino beams to perform long and very long baseline oscillation experiments.

In Ref. [2], we have considered a  $\nu_\mu$  disappearance experiment with a baseline of 730 km. Since the neutrino beams contain both electron and muon flavors, the disappearance of muon neutrino can be performed by directly comparing electron and muon events. This method is self normalizing, i.e. without the need of a near detector to predict the original flux.

Therefore, the very attractive feature for the future, rather than to think of experiments on currently accessible baselines (i.e. the FNAL-NUMI to Soudan and the CERN-NGS to GranSasso) is to imagine a second generation of long baseline experiments with very long baseline of the order of 5000-7000 km, made possible by the intense neutrino sources.



## 2 Oscillation searches at VLBL

The distance  $L$  between neutrino production and detection is a key element in oscillation studies. Since the oscillation probability varies like

$$\sin^2(1.27\Delta m^2(eV^2)L(km)/E_\nu(GeV)),$$

having a longer length means the possibility to explore the same parameter-space region with neutrinos of higher energy.

In addition, since these beams will travel through Earth for thousands of kilometers, matter enhancement in neutrino oscillation [3] can become important, as recently pointed out in Ref. [4]. We perform oscillation searches that can be categorized as follows:

- **$\mu$  disappearance:** similar to what we described in Ref. [2]; but improved due to the larger  $L/E$  ratio, to observe the “dip” in the  $\nu_\mu$  energy distribution, even for the lowest  $\Delta m^2$  suggested by the atmospheric neutrino effect.
- **$e$  and  $\mu$  appearances:** study of matter effects in  $\nu_e \rightarrow \nu_\mu$  oscillations  
Travel through the Earth would enhance the transition probability for neutrinos (antineutrinos) if  $\Delta m^2 > 0$  ( $\Delta m^2 < 0$ ). Running the muon storage ring alternatively with negative and positive muons would directly reveal this effect and determine the sign of  $\Delta m^2$ .
- **$\tau$  appearance:** the production of  $\tau$  leptons can be determined looking for an excess of hadronic events due to hadronic  $\tau$  decays.

We do not consider the possibility of direct tau appearance by identification of the  $\tau$  lepton using kinematical or topological criteria, and postpone it to further studies.

## 3 Possible very long baselines

We assume that a multikiloton detector will be located in Europe at the Laboratori Nazionali del GranSasso (LNGS, Italy).

The ideal detector would be a 10 kiloton (fiducial) SuperICARUS as described in Ref. [5]. In addition to providing excellent spatial resolution like that of bubble-chamber, SuperICARUS, unlike most neutrino detectors, allows for excellent electron identification and measurement. High energy muons, exiting the detector, can also be measured from multiple scattering with a resolution  $\Delta p/p \approx 20\%$ . These unique lepton capabilities are in a sense matched to the beams from muon decays, which provide equal amounts of electron and muon neutrinos.

We also assume that a “sign-determining” muon spectrometer is installed behind the target, to allow the identification of the leading muon charge (“ $\mu^-$ ”, “ $\mu^+$ ” samples). On the other hand, the leading electron charge cannot be identified (“ $e^-$ ” sample). This is due to the fact that electrons will produce a shower soon after production before being sufficiently bent in a possible magnetic field to be measured.

The neutrino source could be located in different laboratories around the world, in the American or Asian continent. For example, we quote BNL-GranSasso ( $L = 5300$  km), FNAL-GranSasso ( $L = 6600$  km), KEK-GranSasso ( $L = 7000$  km).

Our attention was recently drawn to the upgrade of the AGS accelerator in BNL[6]. A total of  $6.6 \times 10^{21}$  protons on target per year could be produced. When used as proton driver of a muon accumulator with a muon yield per proton of 15%, we obtain  $6.6 \times 10^{21} \times 0.15 = 9.9 \times 10^{20}$  muons/year. The machine would be operated for four years, alternating runs with positive and negative muons and we consider that, given the shape of the muon storage ring, half of the muons will decay in the direction towards the GranSasso laboratory. We then use

as integrated intensity a total of

$$N(\mu^+) + N(\mu^-) = \frac{1}{2} \times 6.6 \times 10^{21} \times 0.15 \times 4 \approx 2 \times 10^{21} \mu's$$

decay in the right direction producing neutrinos.

## 4 Event rates for the BNL/AGS-GS baseline

Neutrinos travel the distance between the BNL and GS laboratories and are then detected in the 10 kton (fiducial) detector.

The neutrino event rate will grow as  $E_\mu^3$  where  $E_\mu$  is the energy of the muon storage ring. We are interested in a neutrino beam with energy in the range of 10 – 20 GeV. We list in Table 1 the neutrino event rates in case of no oscillation as a function of the muon storage ring energy, for  $10^{21}$  muons decays of a given charge and 10 kton target. Neutrino interactions have been divided into charged current (CC) and neutral current (NC) interactions. The CC events are split into inelastic scattering (DIS) and quasi-elastic (QE) interactions.

$E_\mu$ (GeV)	$10^{21} \mu^-$ decays			$10^{21} \mu^+$ decays		
	CC( $\bar{\nu}_e$ )	CC( $\nu_\mu$ )	NC	CC( $\nu_e$ )	CC( $\bar{\nu}_\mu$ )	NC
10	648	1752	298	1545	743	263
15	2151	5706	1718	4994	2471	1528
20	5039	13253	5388	11542	5810	4826
25	9408	24554	12053	21376	10851	10877
30	16375	42595	23851	36959	18947	21615

Table 1: The total number of neutrinos detected in a 10 kton (fiducial) detector for a baseline  $L = 5300$  km and a total number of  $10^{21}$  muons decays.

## 5 Neutrino oscillation scenarios

In the preceding section, we have seen that the expected neutrino event rates are comfortable and open possibilities to study various neutrino oscillations scenarios with a baseline of

$$\frac{E}{L} \approx \frac{10 \text{ GeV}}{5300 \text{ km}} \approx 2 \times 10^{-3} \text{ eV}^2.$$

While the atmospheric neutrino evidence is compatible with maximal mixing between  $\nu_\mu$  and  $\nu_\tau$ , it is attractive to think that there is also a smaller mixing between the first and third family. We therefore consider a three-family scenario. The mixing between the different neutrino flavors is determined by two mass differences and a unitary matrix describing the mixing between flavor and mass eigenstates.

We base our computation on the formalism of Ref. [4] and make the approximation that only a mass scale is relevant, i.e. assuming that the differences  $|m_3^2 - m_2^2| \gg |m_2^2 - m_1^2|$  (this approximation being supported by current experimental results on solar neutrinos). The mass eigenstate  $m_1$  is defined orthogonal to the electron flavor state. The mixing matrix takes a form that only depends on the two mixing angles  $\theta$  and  $\phi$ :

$$U = \begin{pmatrix} 0 & \cos \theta & \sin \theta \\ \cos \phi & -\sin \theta \sin \phi & \cos \theta \sin \phi \\ -\sin \phi & -\sin \theta \cos \phi & \cos \theta \cos \phi \end{pmatrix} \quad (1)$$

The three-family oscillation is therefore described by only three parameters: the mass difference between the second and third neutrino  $\Delta m^2 \equiv \Delta m_{23}^2$  and the two mixing angles  $\theta$  and  $\phi$ .

The long travel inside the Earth gives rise to matter effects, resulting in a modification of the oscillation. The mixing angle in matter  $\theta_m$  takes a value given by the expression

$$\sin^2 2\theta_m(x) = \frac{\sin^2 2\theta}{\sin^2 2\theta + (x - \cos 2\theta)^2}$$

and

$$x = \frac{2VE_\nu}{\Delta m^2} = \pm \frac{2\sqrt{2}G_F n_e E_\nu}{\Delta m^2},$$

where the plus sign applies to  $\nu$ 's and the minus to  $\bar{\nu}$ 's and  $n_e$  is the electron density of the medium. In the limit of no matter effects  $x \rightarrow 0$  and the mixing angle  $\theta_m \rightarrow \theta$ . Given the distance between the two laboratories, the beam does not have to go more than 600 m deep, so the electron density of the Earth can be considered constant (see Ref. [7]).

## 6 Oscillated neutrino fluxes

We assume that the mixing is maximal between the second and the third neutrino family ( $\sin^2 \phi = 0.5$ ) and small ( $\sin^2 \theta = 0.025$ ) between the first two. We will consider the three values of  $\Delta m^2 = 10^{-3}, 3 \times 10^{-3}$  and  $10^{-2}$  eV<sup>2</sup>.

In the case of a neutrino beam from negative muons, four oscillation processes will occur:

- $\nu_\mu \rightarrow \nu_e$
- $\nu_\mu \rightarrow \nu_\tau$
- $\bar{\nu}_e \rightarrow \bar{\nu}_\mu$
- $\bar{\nu}_e \rightarrow \bar{\nu}_\tau$

while for the case of positive muons the charge-conjugate processes occur.

The neutrino fluxes as a function of energy for the different flavors in the case of three-family oscillations are shown in Figure 1 for a 20 GeV muon beam and  $\Delta m^2 = 3 \times 10^{-3}$  eV<sup>2</sup>.

## 7 Event classification

We classify the observed events in four classes:

- a) events with electrons or positrons (no electron charge measured),
- b) events with muons of the same sign of those circulating in the storage ring,
- c) events with muons of opposite sign,
- d) events without leptons.

No direct  $\tau$  identification is performed, so, according to their decay,  $\tau$  events are seen either in the electron ( $\tau \rightarrow e$  decays), muon ( $\tau \rightarrow \mu$ ) or neutral current ( $\tau \rightarrow h$ ) sample.

Figure 2 shows the energy spectra of the four classes for a 20 GeV  $\mu^-$  beam. The dotted and full lines refer to the predicted distributions without oscillations, and with oscillations with  $\Delta m^2 = 3 \times 10^{-3}$  eV<sup>2</sup>. In Figure 3 the same distributions are shown for 20 GeV  $\mu^+$  beams.

Let us consider in more detail the processes playing a role for the different classes of observed events. In the following, every process is listed with the relevant probability, where the notation  $P_{\nu_\alpha \rightarrow \nu_\beta}$  is used to identify the probability of neutrinos of flavor  $\alpha$  to oscillate into neutrinos of flavor  $\beta$ . These probabilities (and the text, unless otherwise specified) refer to the case of negative muons in the storage ring; the charge-conjugate must be considered for the case of positive muons.

## 7.1 Events with electrons

In these events, a leading electron or positron is identified in the detector. Such events could be produced by the charged-current interactions of the following neutrinos:

1. unoscillated  $\bar{\nu}_e$  neutrinos from the beam  
 $(1 - P_{\bar{\nu}_e \rightarrow \bar{\nu}_\mu} - P_{\bar{\nu}_e \rightarrow \bar{\nu}_\tau}) \times \Phi_{\bar{\nu}_e}$
2. muon neutrinos oscillated into electron neutrinos  
 $(P_{\nu_\mu \rightarrow \nu_e}) \times \Phi_{\nu_\mu}$
3. tau neutrinos derived from oscillations followed by a  $\tau \rightarrow e$  decay  
 $(P_{\nu_\mu \rightarrow \nu_\tau} \times BR(\tau^- \rightarrow e)) \Phi_{\nu_\mu} + (P_{\bar{\nu}_e \rightarrow \bar{\nu}_\tau} \times BR(\tau^+ \rightarrow e)) \Phi_{\bar{\nu}_e}$

Due to the small mixing between the first and the third family, the most important process for events in this class are  $\nu_\mu \rightarrow \nu_e$  oscillations. In case of  $\mu^-$  beams, process 1) will deplete the number of leading electron events from the beam, while process 2) will increase the number of such events, as they come from oscillation of muon neutrinos. Since process 2) involves neutrinos, it is matter-enhanced, and the net effect will be an increase of the number of observed events having a leading electron with respect to the case of no oscillation, as can be seen comparing the Figures in Table 2 with the non-oscillated case (Table 1).

In the case of  $\mu^+$  beams, the balance of the two competing processes is reversed. Now process 1) involves neutrinos, so the depletion of electron events from the beam is matter-enhanced, while process 2) receives no enhancement. Therefore, in this case the net effect is a smaller number of observed events with leading electrons with respect to the expectations, as can be seen comparing Tables 3 and 1.

$E_\mu$ (GeV)	$\Delta m^2 (eV^2)$	unoscillated beam $(1 - P_{\bar{\nu}_e \rightarrow \bar{\nu}_\mu}) \times \Phi_{\bar{\nu}_e}$	$\nu_\mu \rightarrow \nu_e$ $(P_{\nu_\mu \rightarrow \nu_e}) \times \Phi_{\nu_\mu}$	$\tau$ decay $((P_{\nu_\mu \rightarrow \nu_\tau}) \Phi_{\nu_\mu} + (P_{\bar{\nu}_e \rightarrow \bar{\nu}_\tau}) \Phi_{\bar{\nu}_e})$ $\times BR(\tau \rightarrow e)$
10	$1. \times 10^{-3}$	644	74	19
20		5008	133	119
30		16366	175	262
10	$3. \times 10^{-3}$	630	248	15
20		5005	1124	517
30		16310	1789	1595
10	$1. \times 10^{-2}$	626	48	23
20		4897	553	350
30		15904	5600	861

Table 2: Different contributions to leading electron events from  $\mu^-$  beams.

### 7.1.1 Quasi-elastic events

The electron charge is not measured. In order to identify neutrino or antineutrino interactions without the need of a measurement of the electron charge, quasi-elastic interactions can however be used. In particular,

$$\nu_e + n \rightarrow e^- + p$$

events are quite cleanly distinguishable from DIS processes, due to the presence of a proton, seen in the detector as a highly ionizing track. The same does not hold for antineutrino interactions

$$\bar{\nu}_e + p \rightarrow e^+ + n$$

$E_\mu$ (GeV)	$\Delta m^2(eV^2)$	unoscillated beam $(1 - P_{\nu_e \rightarrow \nu_x}) \times \Phi_{\nu_e}$	$\bar{\nu}_\mu \rightarrow \bar{\nu}_e$ $(P_{\bar{\nu}_\mu \rightarrow \bar{\nu}_e}) \times \Phi_{\bar{\nu}_\mu}$	$\tau$ decay $((P_{\bar{\nu}_\mu \rightarrow \bar{\nu}_\tau})\Phi_{\bar{\nu}_\mu} + (P_{\nu_e \rightarrow \nu_\tau})\Phi_{\nu_e})$ $\times BR(\tau \rightarrow e)$
10	$1. \times 10^{-3}$	1370	3	11
20		11204	15	61
30		36634	30	128
10	$3. \times 10^{-3}$	1173	8	13
20		9163	18	305
30		32931	71	863
10	$1. \times 10^{-2}$	1453	13	11
20		10757	92	160
30		29406	259	717

Table 3: Different contributions to leading electron events from  $\mu^+$  beams.

since the neutrons do not produce any track at the vertex.

The presence of  $e + p$  final state in a beam from  $\mu^-$  is therefore a clear signature for  $\nu_\mu \rightarrow \nu_e$  oscillation. The total rate of  $e^-p$  events produced in quasi-elastic interactions from a beam of negative muons is listed in Table 4. The number of quasi-elastic events is non negligible, even after taking into account the detection efficiency due to a necessary proton momentum threshold for detection and rejection of nuclear spectators protons.

$E_\mu$ (GeV)	$\Delta m^2(eV^2)$	$e^-p$ events (QE) $(P_{\nu_\mu \rightarrow \nu_e}) \times \Phi_{\nu_\mu}$	$e^+n$ events (QE) $(1 - P_{\bar{\nu}_e \rightarrow \bar{\nu}_x}) \times \Phi_{\bar{\nu}_e}$
10	$1. \times 10^{-3}$	9	88
20		10	390
30		10	888
10	$3. \times 10^{-3}$	21	86
20		61	389
30		75	885
10	$1. \times 10^{-2}$	5	86
20		26	381
30		165	863

Table 4: Number of quasi-elastic interactions ( $e^-p$  final states) from neutrinos produced in  $\mu^-$  beams

## 7.2 Events with right-sign muons

The muon charge is measured by a spectrometer placed behind the detector. Muons of the same sign of those decaying in the storage ring are produced by:

1. muon neutrinos coming from the beam

$$(1 - P_{\nu_\mu \rightarrow \nu_e} - P_{\nu_\mu \rightarrow \nu_\tau}) \times \Phi_{\nu_\mu}$$

2.  $\tau$  decays, where the  $\tau$  is coming from  $\nu_\mu \rightarrow \nu_\tau$  or  $\bar{\nu}_e \rightarrow \bar{\nu}_\tau$  oscillations.

$$P_{\nu_\mu \rightarrow \nu_\tau} \times BR(\tau \rightarrow \mu) \times \Phi_{\nu_\mu} + P_{\bar{\nu}_e \rightarrow \bar{\nu}_\tau} \times BR(\tau \rightarrow \mu) \times \Phi_{\bar{\nu}_e}$$

Since in this case we measure the muon sign,  $\nu_\mu$  oscillating into  $\nu_e$  are not compensated by  $\bar{\nu}_e$  oscillations into  $\bar{\nu}_\mu$ , as they produce muons of opposite charge (see following subsection). A

small compensation to the total number of right-sign muons comes from  $\nu_\mu \rightarrow \nu_\tau$  oscillations where the  $\tau$  decays into a muon. For both  $\mu^-$  and  $\mu^+$  events, the net effect of neutrino oscillations is a disappearance of right-sign leading muon events.

### 7.3 Events with wrong-sign muons

Opposite-sign muons can only be produced by neutrino oscillations, since there is no component in the beam that could account for them. These events are coming from oscillations of the electron component of the beam:

1. directly via  $\bar{\nu}_e \rightarrow \bar{\nu}_\mu$  oscillations

$$P_{\bar{\nu}_e \rightarrow \bar{\nu}_\mu} \times \Phi_{\bar{\nu}_e}$$

2. via  $\tau$  decays after  $\bar{\nu}_e \rightarrow \bar{\nu}_\tau$  oscillations.

$$P_{\bar{\nu}_e \rightarrow \bar{\nu}_\tau} \times BR(\tau \rightarrow \mu) \times \Phi_{\bar{\nu}_e}$$

Opposite sign muons could be produced in decays of hadrons in neutral current events. We note however that these muons will be soft and not isolated from the jet and can therefore be suppressed by a mild isolation and momentum cut.

For reasons opposite to those already explained in the discussion of events with leading electrons, the production of events opposite-sign muons is suppressed in beams from  $\mu^-$  decays, and enhanced in beams from  $\mu^+$  decays. Since this enhancement is due to the presence of matter, the energy spectrum of these events has a peak close to the resonance energy (about 13 GeV for  $\Delta m^2 = 3 \times 10^{-3} eV^2$ ).

The number of events for both same-sign and wrong-sign muons are shown in Tables 5 and 6.

$E_\mu$ (GeV)	$\Delta m^2 (eV^2)$	$\bar{\nu}_e \rightarrow \bar{\nu}_\mu$ $\mu^+$	$\bar{\nu}_e \rightarrow \bar{\nu}_\tau$ $\mu^+$	unoscillated beam $\mu^-$	$\nu_\mu \rightarrow \nu_\tau$ $\mu^-$
10.	$1. \times 10^{-3}$	2	0	711	19
20.		15	1	10362	118
30.		31	2	38080	260
10.	$3. \times 10^{-3}$	9	0	846	15
20.		16	1	2264	517
30.		59	4	17389	1591
10.	$1. \times 10^{-2}$	11	0	713	22
20.		70	3	5745	347
30.		262	17	24352	844

Table 5: Different contributions to leading-muon events from  $\mu^-$  beams

### 7.4 Events with no leading leptons

Events with no leading leptons can be produced in

1. neutral current processes
2. hadronic  $\tau$  decays

$$P_{\nu_\mu \rightarrow \nu_\tau} \times BR(\tau \rightarrow hadrons) \times \Phi_{\nu_\mu} + P_{\bar{\nu}_e \rightarrow \bar{\nu}_\tau} \times BR(\tau \rightarrow hadrons) \times \Phi_{\bar{\nu}_e}$$

The neutral current processes do not depend on the oscillations, so there is always an excess of events in this class, due to the hadronic  $\tau$  decays, with respect to the expectation.

Total number of events for these two categories is shown in Table 7, for both  $\mu^-$  and  $\mu^+$  beams.

$E_\mu$ (GeV)	$\Delta m^2 (eV^2)$	$\nu_e \rightarrow \nu_\mu$ $\mu^-$	$\nu_e \rightarrow \nu_\tau$ $\mu^-$	unoscillated beam $\mu^+$	$\bar{\nu}_\mu \rightarrow \bar{\nu}_\tau$ $\mu^+$
10.	$1. \times 10^{-3}$	88	1	301	10
20.		168	5	4548	56
30.		222	10	16949	118
10.	$1. \times 10^{-3}$	186	4	403	9
20.		1188	49	995	257
30.		2073	112	7706	751
10.	$1. \times 10^{-3}$	46	1	318	10
20.		391	17	2884	143
30.		3834	273	12229	444

Table 6: Different contributions to leading-muon events from  $\mu^+$  beams

$E_\mu$ (GeV)	$\Delta m^2 (eV^2)$	$\mu^-$ beam		$\mu^+$ beam	
		NC	$\tau \rightarrow$ hadrons	NC	$\tau \rightarrow$ hadrons
10.	$1. \times 10^{-3}$	298	73	263	41
20.		5375	455	4819	233
30.		23877	1000	21680	490
10.	$3. \times 10^{-3}$	298	58	263	49
20.		5375	1977	4819	1167
30.		23877	6097	21680	3301
10.	$3. \times 10^{-3}$	298	87	263	43
20.		5375	1339	4819	614
30.		23877	3292	21680	2743

Table 7: Different contributions to events with no leading leptons.

## 8 Ratios of observed versus expected events

Given the large oscillation probabilities, the oscillation signatures will appear strongly. We illustrate this by computing the ratios of observed over expected events for the four classes. These numbers are shown in Tables 8 and 9 with their statistical error. In all cases, the effect is significant; to increase further the electron case, it is possible to take the double ratio between events detected with negative and positive muons.

In order to measure the oscillation parameters, it is interesting to notice the dependence on  $\Delta m^2$  of the energy spectrum of wrong-sign muons. The position of the peak of the distribution depends on the resonance energy, which is a function of  $\Delta m^2$ . In Figure 4 this distribution is shown for  $\Delta m^2$  values of 1, 2, 3,  $4 \times 10^{-3}$  eV<sup>2</sup>.

## 9 Interpretation of experimental results

A fit to the observed energy distributions and rates allows the determination of the parameters  $\Delta m^2$ ,  $\theta$  and  $\phi$  governing the oscillation; the fit probability is a test of the hypothesis that one mass scale is relevant, and that there are no other processes or phenomena (i.e. sterile neutrinos). Given the statistical accuracies obtained in Tables 8 and 9, we foresee that these fits will give good constraints on the oscillation parameters and scenarios.

$E_\mu$ (GeV)	$\Delta m^2 (eV^2)$	$\nu_e + \bar{\nu}_e / \bar{\nu}_e^{EXP.}$	$\nu_\mu / \nu_\mu^{EXP.}$	$\bar{\nu}_\mu / \nu_\mu^{EXP.}$	$NC / NC^{EXP}$
10.0	$1. \times 10^{-3}$	$1.137 \pm 0.042$	$0.417 \pm 0.0155$	$0.0014 \pm 0.0010$	$1.245 \pm 0.065$
20.0		$1.044 \pm 0.015$	$0.792 \pm 0.0078$	$0.0012 \pm 0.0004$	$1.085 \pm 0.015$
30.0		$1.023 \pm 0.008$	$0.900 \pm 0.0046$	$0.0008 \pm 0.0002$	$1.042 \pm 0.007$
10.0	$3. \times 10^{-3}$	$1.379 \pm 0.047$	$0.491 \pm 0.0168$	$0.0052 \pm 0.0017$	$1.195 \pm 0.063$
20.0		$1.319 \pm 0.016$	$0.210 \pm 0.0040$	$0.0013 \pm 0.0004$	$1.368 \pm 0.016$
30.0		$1.199 \pm 0.009$	$0.446 \pm 0.0033$	$0.0015 \pm 0.0003$	$1.255 \pm 0.007$
10.0	$1. \times 10^{-2}$	$1.074 \pm 0.041$	$0.420 \pm 0.0155$	$0.0066 \pm 0.0019$	$1.290 \pm 0.066$
20.0		$1.151 \pm 0.015$	$0.461 \pm 0.0059$	$0.0055 \pm 0.0009$	$1.249 \pm 0.015$
30.0		$1.361 \pm 0.010$	$0.592 \pm 0.0038$	$0.0065 \pm 0.0006$	$1.138 \pm 0.007$

Table 8: Ratio between the events observed in each class for negative muon decays, and the events that would be observed without oscillation. Errors are statistical only

$E_\mu$ (GeV)	$\Delta m^2 (eV^2)$	$\nu_e + \bar{\nu}_e / \nu_e^{EXP.}$	$\nu_\mu / \bar{\nu}_\mu^{EXP.}$	$\bar{\nu}_\mu / \bar{\nu}_\mu^{EXP.}$	$NC / NC^{EXP}$
10.0	$1. \times 10^{-3}$	$0.895 \pm 0.025$	$0.419 \pm 0.0243$	$0.1196 \pm 0.0130$	$1.157 \pm 0.068$
20.0		$0.978 \pm 0.009$	$0.794 \pm 0.0120$	$0.0298 \pm 0.0023$	$1.048 \pm 0.015$
30.0		$0.992 \pm 0.005$	$0.901 \pm 0.0071$	$0.0122 \pm 0.0009$	$1.023 \pm 0.007$
10.0	$3. \times 10^{-3}$	$0.773 \pm 0.023$	$0.554 \pm 0.0280$	$0.2558 \pm 0.0190$	$1.186 \pm 0.069$
20.0		$0.822 \pm 0.009$	$0.216 \pm 0.0062$	$0.2133 \pm 0.0062$	$1.242 \pm 0.016$
30.0		$0.913 \pm 0.005$	$0.446 \pm 0.0050$	$0.1154 \pm 0.0026$	$1.152 \pm 0.008$
10.0	$1. \times 10^{-2}$	$0.956 \pm 0.026$	$0.443 \pm 0.0250$	$0.0631 \pm 0.0094$	$1.163 \pm 0.068$
20.0		$0.954 \pm 0.009$	$0.522 \pm 0.0097$	$0.0704 \pm 0.0035$	$1.127 \pm 0.016$
30.0		$0.820 \pm 0.005$	$0.669 \pm 0.0061$	$0.2168 \pm 0.0035$	$1.127 \pm 0.007$

Table 9: Same as previous Table, but for the decay of positive muons.

## 10 Conclusions

The possibility of performing a second generation very-long baseline experiment using an intense neutrino beam from negative and positive muons offers the unique opportunity to study the  $\Delta m^2$  region indicated by the atmospheric neutrinos. At the chosen optimized  $L/E$  distance, the oscillation probabilities are maximized and will allow a complete understanding of the oscillation parameters governing the  $\nu_\mu \rightarrow \nu_\tau$  oscillation. Even in the case where a simple counting experiment is performed like the one we have assumed, the visible effects are significant. A large disappearance of muon neutrinos not compensated by the appearance of taus — e.g.  $\nu_\mu \rightarrow \nu_s$  — would be immediately noticed. In addition, the unique feature of the muon decay beams providing electron and muon neutrinos in same quantities, allow the study matter effects in Earth and given the distance and energies involved should reveal directly the presence of the oscillation resonance. By a change of sign in the muon storage ring, the matter effects can be studied by directly comparing the oscillations of neutrinos and their anti-neutrinos.

## Acknowledgments

We are indebted to R. Palmer for enlighting us on the possible upgrade of the AGS at BNL.



## References

- [1] A.Bueno, M.Campanelli, A.Rubbia “A medium baseline search for  $\nu_\mu \rightarrow \nu_e$  oscillations at a  $\nu$  beam from muon decays” hep-ph/9809252 CERN-EP/98-140 accepted by IJMP.
- [2] A.Bueno, M.Campanelli, A.Rubbia “Long baseline neutrino oscillation disappearance search using a  $\nu$  beam from muon decays” hep-ph/9808485 ETHZ-IPP-98-05 accepted by IJMP.
- [3] L. Wolfenstein, Phys. Rev. **D17**, 2369 (1978); Phys. Rev. **D 20**, 2634 (1979); Mikheyev and Smirnov, Sov.J.Nucl.Phys. **42**, 913 (1986).
- [4] P.Lipari, hep-ph/9903481.
- [5] ICARUS collaboration, “*ICARUS-Like Technology for Long Baseline Neutrino Oscillations*”, CERN/SPSC/98-33 & M620, 1998 and references therein.
- [6] Robert Palmer and Thomas Roser, private communications.
- [7] J. Bahcall, P. Krastev, Phys. Rev. **C56** 2839-2857, 1997.

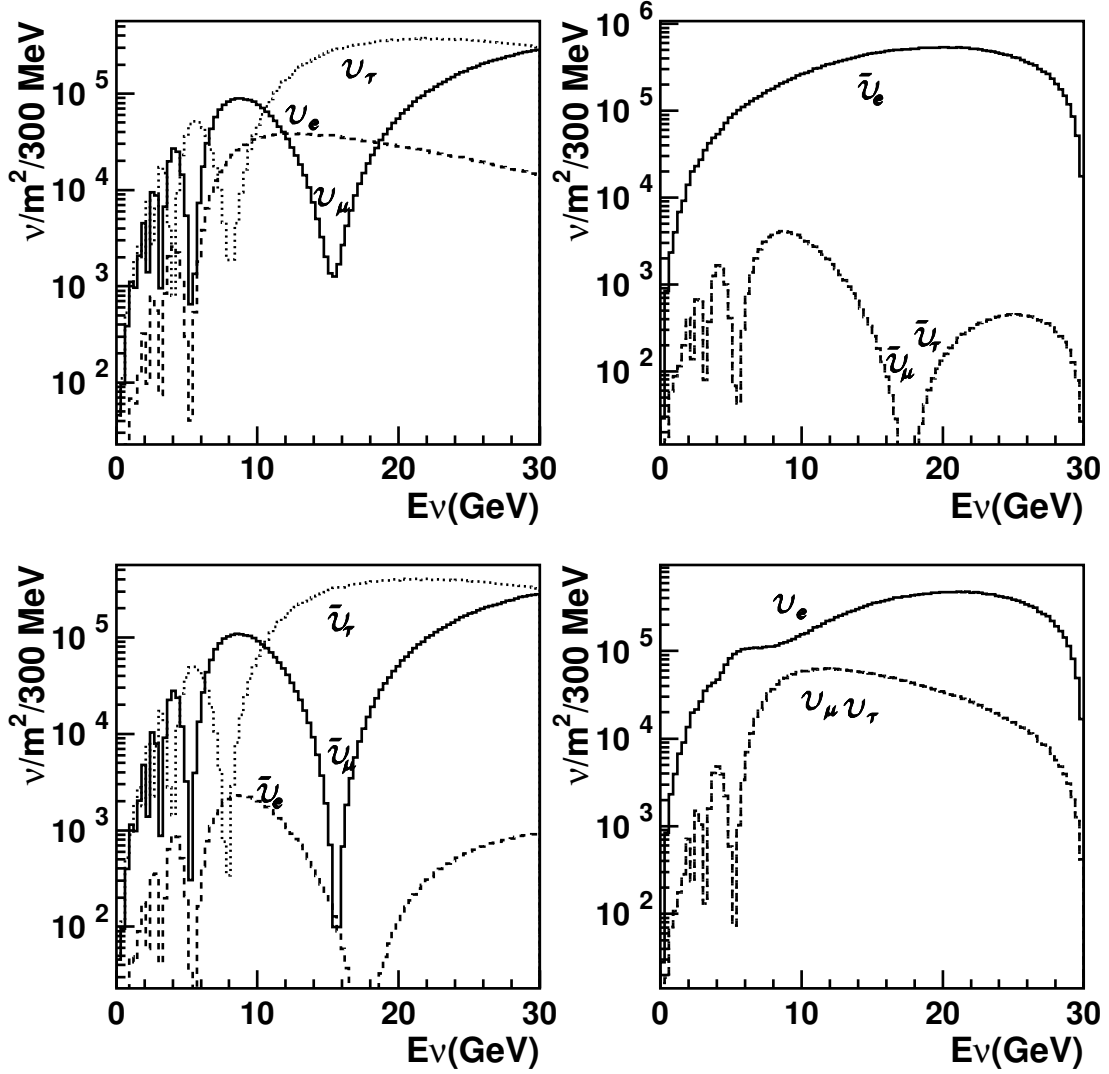


Figure 1: Neutrinos per  $m^2$  reaching the detector for three-family mixing with  $\Delta m^2 = 3 \times 10^{-3} eV^2$ ,  $\sin^2 \phi = 0.5$ ,  $\sin^2 \theta = 0.025$ . The two upper plots refer to a run with 20 GeV  $\mu^-$ , the two lower to a run with 20 GeV  $\mu^+$ .

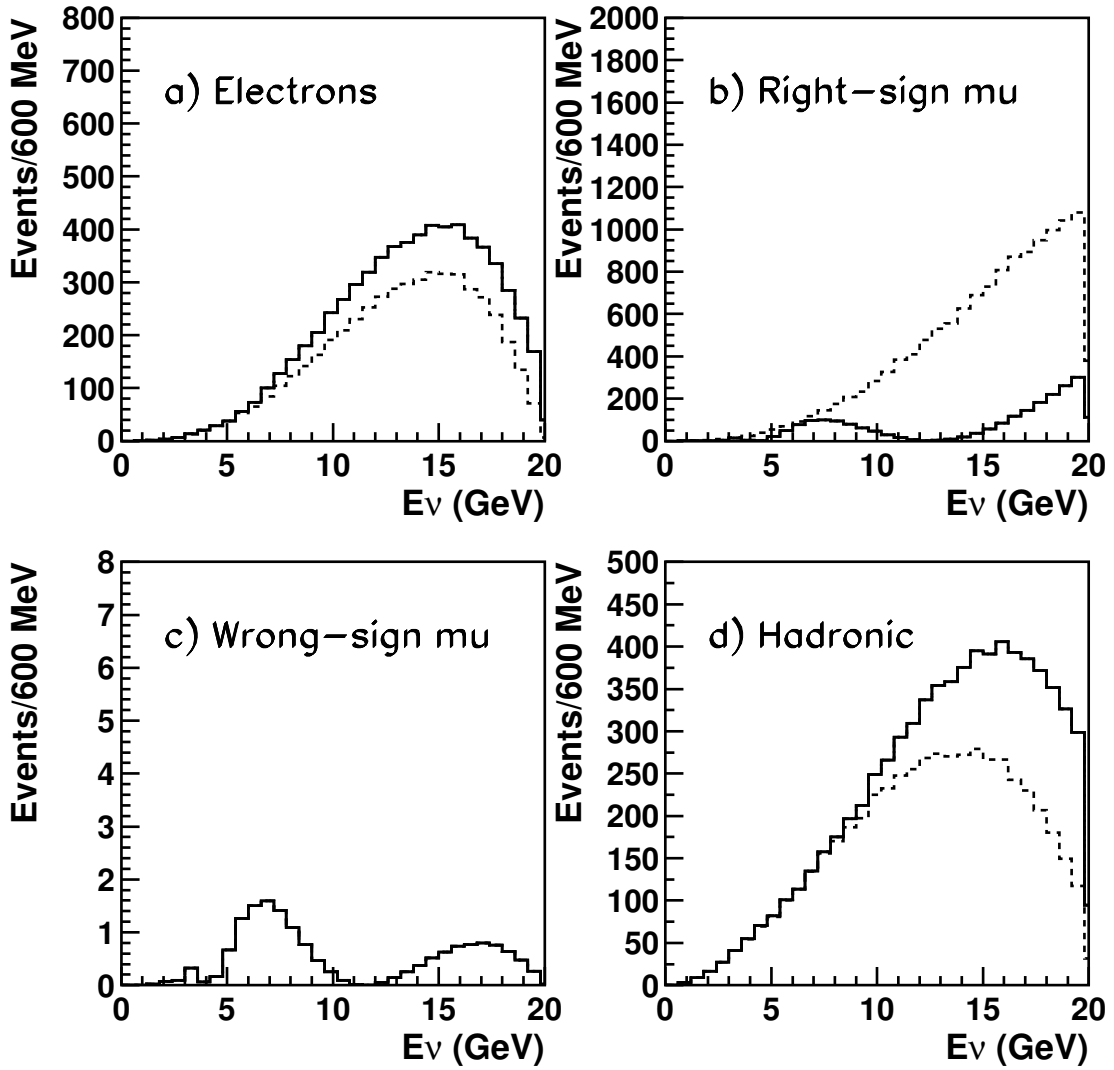


Figure 2: Neutrino energy spectra corresponding to 20 GeV  $\mu^-$  decays, for a target mass of 10 kton. Full line: spectra with oscillations; dashed line: spectra without oscillations. a) events with leading electron or positron, b) events with leading  $\mu^-$ , c) events with leading  $\mu^+$  d) events with no leading leptons.

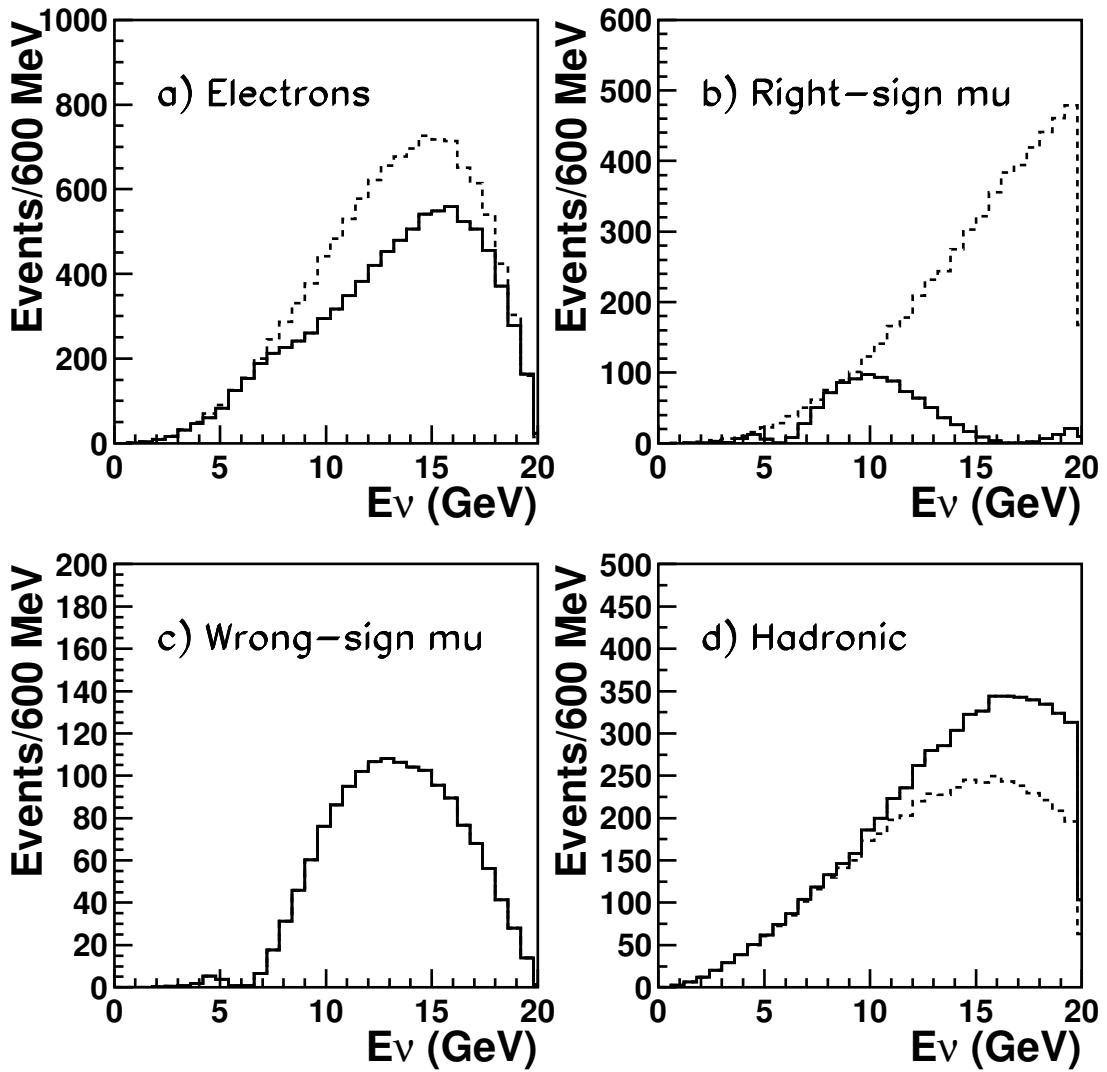


Figure 3: Same as previous plot, but  $20 \text{ GeV } \mu^+$  decays. The sign of the muon charges are also exchanged, i.e. plot b refers to events with leading  $\mu^+$ , plot c to events with leading  $\mu^-$ .

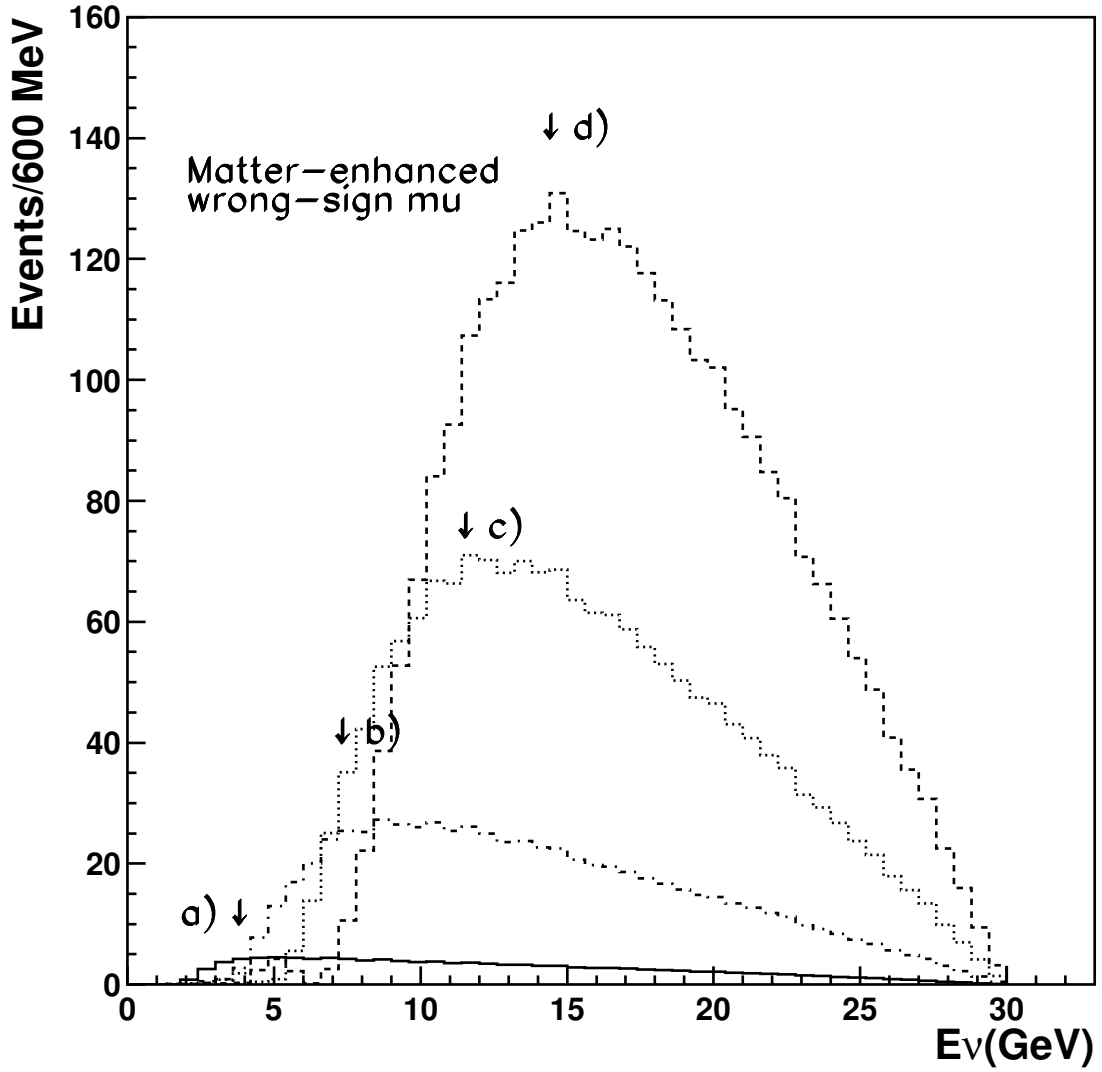


Figure 4: Energy spectra of events with leading  $\mu^-$  in a decay beam of positive muons. The different distributions refer to the following values of  $\Delta m^2(eV^2)$ : a)  $1 \times 10^{-3}$ , b)  $2 \times 10^{-3}$ , c)  $3 \times 10^{-3}$ , d)  $4 \times 10^{-3}$ . The shift in the peak position, corresponding to the resonance of oscillations due to matter effects (indicated by an arrow) is clearly visible.